

Unitarized pion-nucleon scattering within Heavy Baryon Chiral Perturbation Theory

A. Gómez Nicola and J. R. Peláez

Departamento de Física Teórica.

Universidad Complutense. 28040 Madrid. SPAIN.

February 27, 2019

Abstract

By means of the Inverse Amplitude Method we unitarize the elastic pion-nucleon scattering amplitudes obtained from Heavy Baryon Chiral Perturbation Theory to $\mathcal{O}(q^3)$. Within this approach we can enlarge their applicability range and generate the $\Delta(1232)$ resonance. We can find a reasonable description of the pion nucleon phase shifts with $\mathcal{O}(q^2)$ parameters in agreement with the resonance saturation hypothesis. However, the uncertainties in the analysis of the low energy data as well as the large number of chiral parameters, which can have strong correlations, allow us to obtain very good fits with rather different sets of chiral constants.

1 Introduction

Chiral Symmetry plays a fundamental role in the interactions between pions and nucleons, as it was already well known in the sixties, when current algebra was used to describe many hadron observables. However, in order to go beyond current algebra or tree level calculations from simple phenomenological models, one needs an effective low-energy field theory with all the QCD symmetries and a systematic power counting. Heavy Baryon Chiral Perturbation Theory (HBChPT) [1] is the best candidate to date for such an effective theory. For the case of two light flavors, the HBChPT degrees of freedom (in its minimal formulation) are the nucleons and pions, which obey an $SU(2)$ chiral symmetry. The pions are the Nambu-Goldstone bosons associated to the spontaneous chiral symmetry breaking, whereas the nucleons are included as an isospin doublet. In the case of $SU(3)$ symmetry, the pseudoscalar meson and baryon octets are the minimal set of fields required to describe the meson-baryon sector. One should point out that non-minimal formulations have also been developed, including also the baryon decuplet as a fundamental field in the effective Lagrangian [2]. In this paper, we will restrict to the minimal case for an $SU(2)$ symmetry, although later on we will comment about possible extensions of our approach.

The HBChPT Lagrangian is built as an expansion in derivatives and meson masses, including all possible terms compatible with the chiral symmetry. In fact, the HBChPT

philosophy is the same as that originally followed in pure meson Chiral Perturbation Theory (ChPT) [3]. However, one should note at least two important differences between them. First, the scale with respect to which one expands in HBChPT is not only the typical chiral symmetry breaking scale of pion loops $\Lambda_\chi = 4\pi f_\pi \simeq 1.2$ GeV, but also the mass of the nucleons. Second, when dealing with baryons, one has to face the difficulty that the nucleon four-momentum is of the same order as the expansion scale, since its mass is $m_B \simeq 1$ GeV, no matter how small is the momentum transfer, and even in the chiral limit [4]. HBChPT circumvents this problem by treating the mass of the nucleons as large compared to the external momenta and redefining their fields in terms of velocity-dependent eigenstates satisfying a massless Dirac equation. In fact, an slightly off-shell baryon four-momentum p can be written as:

$$p^\mu = m_B v^\mu + k^\mu \quad (1)$$

with $v \cdot k \ll m_B$, v being the nucleon velocity. Therefore, one can define v -dependent baryon fields as

$$B_v(x) = \frac{1+\not{v}}{2} \exp(im_B \not{v} v_\mu x^\mu) B(x) \quad (2)$$

satisfying now a *massless* Dirac equation $\not{\partial} B_v = 0$ and whose momenta is $k \ll m_B$. The anti-baryon components can be integrated out [5]. Lorentz invariance is ensured by integrating with a Lorentz invariant measure, i.e. $\mathcal{L} = \int \frac{dv^3}{2v^0} \mathcal{L}_v$. This procedure follows the ideas of Heavy Quark Effective Theory [6]. Once this is done, it is possible to find a *systematic* power counting in k/Λ_χ , k/m_B , q/Λ_χ and q/m_B , where q stands for any meson mass or external momentum. Generically we will denote all these small quantities as $\mathcal{O}(q)$.

With the vertices of the Effective Lagrangian up to a given order, one has to calculate Feynman diagrams containing loops. Each loop increases the order of the diagram so that any loop divergence can be absorbed by renormalising the coefficients of higher order operators. Such coefficients are unknown and have to be fitted to experiment. It is therefore possible to obtain finite results order by order for any observable in HBChPT, but paying the price of introducing more chiral parameters. In particular, the full HBChPT Lagrangian up to $\mathcal{O}(q^3)$ has been given in [7, 8]. It involves 5 unknown coefficients to $\mathcal{O}(q^2)$ and 23 more to $\mathcal{O}(q^3)$.

In this paper, we will concentrate on the pion-nucleon scattering amplitude. We will start from the amplitude derived from minimal HBChPT to $\mathcal{O}(q^3)$ and, by means of the Inverse Amplitude Method (IAM), we will obtain a unitarized amplitude which not only fits the data to higher energies than HBChPT but also reproduces the $\Delta(1232)$ resonance. The structure of the paper is the following. In section 2, we will very briefly review the known results for the HBChPT πN scattering amplitude and we will introduce the basic notation. Our method for unitarizing the amplitude will be introduced in section 3, whereas section 4 will be devoted to explain the results we have obtained with different methods of fitting the data. Finally, in section 5 we will summarize the main conclusions of this work and discuss the limitations and possible extensions of our approach.

Table 1: Combinations of chiral constants appearing in $\mathcal{O}(q^3)$ $\pi - N$ scattering.

	a_1	a_2	a_3	a_5	$b_1 + b_2$	b_3	b_6	$b_{16} - b_{15}$	b_{19}
HBChPT fit to extr. threshold parameters [10]	-2.6	1.4	-1.0	3.3	2.4	-2.8	1.4	6.1	-2.4
HBChPT fit to low-energy phase shifts [8]	-3	1.4	-1.5	3.4	2.7	-3.1	0.4	5.7	-0.8
Resonance Saturation [9]	$-2.6^{+0.4}_{-0.0}$	$1.7^{+0.1}_{-0.5}$	-0.9 (input)	$3.6^{+0.0}_{-0.6}$	-	-	-	-	-

2 HBChPT amplitudes for π -N scattering

In the last few years, and despite its difficulty, several works related to the HBChPT πN scattering amplitude have appeared in the literature [8, 9, 10]. In this work we will follow the notation of the first complete result for the π -N scattering amplitude to $\mathcal{O}(q^3)$, which has been given in [10]. Thus, we are denoting by a_i and b_i the $\mathcal{O}(q^2)$ and $\mathcal{O}(q^3)$ parameters, respectively. The equivalence between this notation and that of [8, 9] can be found, for instance, in [8].

Only four $\mathcal{O}(q^2)$ and five $\mathcal{O}(q^3)$ combinations of all the chiral parameters appearing in the HBChPT Lagrangian, are relevant for the π -N scattering amplitude. We have listed in Table 1 the results of different ways of fitting the values of those parameters in the literature: On the one hand, in [10], the *extrapolated* threshold values of [11], together with the nuclear σ -term and the Goldberger-Treiman discrepancy were taken as the experimental input. On the other hand, in [8] the S and P -wave phase shifts, somewhat away from threshold, were used as data for the fits. The phase shifts can be obtained, for instance, from [12], although they have to be interpreted cautiously since they are not really experimental data. Indeed, they are an extrapolation from real data. Also in [13] it is suggested that the data in [12] yields a too large σ term when analyzed with HBChPT.

As pointed out by their authors, both procedures are subject to some caveats, either because of the many uncertainties of the data near threshold (see comments in [8] and references therein), or because the errors for the extrapolated phase shifts are clearly underestimated (see comments in [10]). For that reason we have not quoted any error in the first two rows of Table 1.

Concerning theoretical estimates of the chiral parameters, in [9] it was suggested that the a_i could be understood in terms of resonance exchange saturation. We give the estimated values in the third row of Table 1. Further constraints from dispersive techniques can be found in [13]. In general, there is a fairly good agreement between the determinations of the dimension two constants, a_i , but that is not the case for those of dimension three, b_i (see comments in [13]).

In addition, one should stress that the predictions obtained within this framework are promising, although not as impressive near threshold [10] as those of standard ChPT

for mesons. As any other effective theory it is limited to low pion momentum, and with the presently available calculations certainly below $q_\pi \lesssim 200$ MeV [8]. The reason for this limitations is, basically, that the convergence of HBChPT is rather slow. As a matter of fact, the contributions of the first three orders are frequently comparable.

In order to improve this situation, we could perform the next order calculation, although then we would have to deal with many more parameters, loosing predictive power. It is even possible to introduce further explicit degrees of freedom, like the lightest resonances [14], but that would also increase the number of parameters. It should be noticed that the introduction of explicit resonances in an effective Lagrangian may improve the unitarity behavior. However, even with such explicit resonance fields, some kind of unitarization should also be carried out to impose strict unitarity. This approach has been followed very recently [15], by introducing explicitly the $\Delta(1332)$ and the Roper $N^*(1440)$ resonances, together with the tree level contributions from lowest order HBChPT. These amplitudes are then unitarized with the N/D method yielding remarkable results for the $\pi - N$ phase shifts.

An alternative approach is the one proposed here, where, encouraged by the HBChPT results commented above, and by the success of unitarization techniques in meson-meson scattering [16, 17], we expect to extend the applicability of HBChPT to higher energies by implementing unitarity. However, *we will not introduce any additional field*. Before that, let us briefly sketch the basic notation needed for our purposes.

Customarily [18], the π -N scattering amplitude $\pi^a(q) + N(mv + p, \sigma) \rightarrow \pi^b(q') + N(mv + p', \sigma')$ is separated into isoscalar and isovector parts defined from

$$T^{ab} = T^+ \delta^{ab} - T^- i \epsilon^{abc} \tau^c, \quad (3)$$

where ϵ^{abc} is the Levi-Civita tensor. Both T^+ and T^- can also be parametrized as follows:

$$T^\pm = \bar{u}(mv + p', \sigma') \left(A^\pm(s, t, u) + B^\pm(s, t, u) \frac{\not{q} + \not{q}'}{2} \right) u(mv + p', \sigma'). \quad (4)$$

For our purposes, it is more convenient to use the isospin basis and define the $1/2$ and $3/2$ total isospin amplitudes

$$\begin{aligned} T^{I=1/2} &= T^+ + 2T^-, \\ T^{I=3/2} &= T^+ - T^-, \end{aligned}$$

and similarly for A^I and B^I . Parity and total angular momentum J conservation implies the conservation of the orbital angular momentum L and thus the analysis of the experimental data are usually presented in terms of partial waves, defined as

$$\begin{aligned} f_{L,J=L\pm 1/2}^I(\sqrt{s}) &= \frac{1}{16\pi\sqrt{s}} \int_{-1}^1 d\cos\theta \left\{ (E + m_N) \left[A^I(s, \theta) \right. \right. \\ &\quad + \left. \left. (\sqrt{s} - m_N) B^I(s, \theta) \right] P_L(\cos\theta) \right. \\ &\quad - \left. (E - m_N) \left[A^I(s, \theta) - (\sqrt{s} + m_N) B^I(s, \theta) \right] P_{L\pm 1}(\cos\theta) \right\} \end{aligned}$$

where $P_L(x)$ are the Legendre polynomials. Finally, the spectroscopic notation $L_{2I+1,2J+1}$ (with $L = S, P, \dots$ waves) is also frequently used to refer to partial waves, and so we will do in our results.

3 The IAM applied to π -N scattering.

Unitarization methods are not foreign to effective theories. Indeed, it is well known that Padé approximants, together with very simple phenomenological models are enough to describe the main features of π -N scattering (see [19] and references therein). Although a systematic application within an effective Lagrangian approach was called for, it was never carried out.

As we have already commented, within the HBChPT formalism, the π -N amplitudes, and in particular the partial waves, are obtained as a series in the momentum transfer and meson masses. One would therefore expect to find expressions which are basically made of polynomials in the energy and mass variables as well as logarithms from the loops. These logarithms provide the analytic cuts and the imaginary parts required by unitarity. However, such an expansion will never satisfy the *exact* π -N *elastic* unitarity condition

$$\text{Im } t = q_{cm} |t|^2, \quad (5)$$

with q_{cm} the momentum of the incoming pion in the center of mass system. Nevertheless HBChPT should satisfy unitarity *perturbatively*, in the following sense:

$$\begin{aligned} \text{Im } t_1 &= 0. \\ \text{Im } t_2 &= 0. \\ \text{Im } t_3 &= q_{cm} |t_1|^2. \end{aligned} \quad (6)$$

where t_k stands for the $\mathcal{O}(q^k)$ contribution to the amplitude. This is indeed the case of the calculations in [8], but not of those in [10], where an additional redefinition of the nucleon field has been performed in order to eliminate the $(v \cdot \nabla)^2/2m$ terms in the Lagrangian [7]. Clearly, the definition of the t_k above varies according to the higher order terms one retains to a given order in q . However, it is always possible to carry out an additional $1/m$ expansion of the results in [10] and recover a pure expansion satisfying eq.(6). In other words, such an expansion retains *only* the $\mathcal{O}(q^k)$ in t_k and not the higher orders. For that purpose, we have counted q_{cm} and M as $\mathcal{O}(\epsilon)$, so that each partial wave reads $t \simeq t_1 + t_2 + t_3 + \mathcal{O}(\epsilon^4)$, where the subscript stands for the order ϵ of each contribution. We have explicitly checked that in this way eq.(6) is verified.

Unfortunately, an energy expansion is not able to accommodate unitarity saturation effects and resonances with their associated poles, which are relevant features of strong interactions. Of course, it is always possible to include them explicitly in an effective Lagrangian, as it has been done, for instance, with the $\Delta(1232)$ and $N^*(1440)$ in [14] reproducing the phase shifts up to $q_\pi \simeq 100$ MeV. If, in addition, these amplitudes are unitarized with, for instance, the N/D method, the agreement is rather good up to $\sqrt{s} \simeq 1350$ MeV [15]. Our approach here will be different, and we will try to make use of the fact that the values of the constants in the minimal HBChPT Lagrangian should carry the information on the underlying dynamics and, in particular, on heavier states. As commented above, it also seems that the a_i values are basically determined from a few resonances [9]. Our purpose here is to unitarize the amplitudes, extending the HBChPT applicability to higher energies and then to see whether the resonances can be reproduced with the resulting amplitudes. For that purpose, we will use the IAM that we describe next.

Let us recast the unitarity condition in a more convenient form. We first divide eq.(5) by $|t|^2$, to get

$$\text{Im} \frac{1}{t} = -q_{cm} \implies \frac{1}{t} = \text{Re} \frac{1}{t} - i q_{cm}. \quad (7)$$

Therefore, any amplitude that satisfies elastic unitarity should have *exactly* the following form:

$$t = \frac{1}{\text{Re}(1/t) - i q_{cm}}. \quad (8)$$

for physical values of the energy, and below any inelastic threshold. The problem, of course, is how to obtain the real part of the inverse amplitude. For instance, setting $\text{Re}(1/t) = |q_{cm}| \cot\delta = -\frac{1}{a} + \frac{r_0}{2} q_{cm}^2$ we reobtain the familiar effective range approximation, whereas by taking $\text{Re} t \simeq t_1$ we arrive at a Lippmann-Schwinger type equation [17]. A frequent criticism to unitarization methods is that they cannot be trusted since apparently they yield different results. However, from the point of view of eq.(8) we see that what really makes two unitarization methods different is the way of approximating $\text{Re}(1/t)$. Therefore it is possible to compare two different techniques and decide which one is better or more trustable, according on how good is the approximation chosen for $\text{Re}(1/t)$. In fact, once we have identified the approximation method, it would be possible to improve them and get an even better amplitude.

Since we want to restrict our Lagrangian to include just pions and nucleons preserving the $SU(2)$ chiral symmetry, the most general way of approximating $\text{Re}(1/t)$ is to use HBChPT. In particular, we will make use of the $\mathcal{O}(q^3)$ calculations above mentioned, but the method can be easily generalized to higher orders. Therefore, we arrive at

$$t \simeq \frac{t_1^2}{t_1 - t_2 + t_2^2/t_1 - \text{Re} t_3 - i q_{cm} t_1^2}, \quad (9)$$

where we have retained only the relevant order in $\text{Re}[(t_1 + t_2 + t_3)^{-1}]$. This is the $\mathcal{O}(q^3)$ form of the IAM. Note that if we expand again in terms of q , we recover at low energies the HBChPT result. Nevertheless, the amplitude satisfies elastic unitarity, which in particular implies that t does not grow with energy. For those more familiar with the K matrix approach, what we have done is to identify $K^{-1} = \text{Re} t^{-1}$. Incidentally, eq.(9) is nothing but a Padé approximant of the $\mathcal{O}(q^3)$ series.

Let us now remark that in the derivation of the IAM we have made use of the elastic unitarity condition, which is only satisfied for real values of s above threshold. However, the extension of the IAM formula to the complex plane can be justified using dispersion relations [16], provided one is not very far from the physical cut, although in other regions (around the left cut for instance) the IAM formula would be inappropriate. As a consequence, it is also possible to reproduce the poles in the second Riemann sheet, which are close to the physical cut and are associated to resonances. As a matter of fact, with the advent of ChPT, the IAM has been successfully applied to meson-meson scattering [16]. In particular, using the $\mathcal{O}(p^4)$ ChPT Lagrangian, the IAM generalized to coupled channels yields a remarkable description of all channels up to about 1.2 GeV, including the σ , f_0 , a_0 , ρ , κ , K^* and octet ϕ resonances [17]. In the meson-nucleon sector, the Lippmann-Schwinger type equation mentioned above has been used to describe the S-wave kaon-nucleon scattering, with eight coupled channels, using the lowest order

Lagrangian plus one parameter [20], reproducing all the low energy cross-sections as well as the $\Lambda(1405)$ resonance.

4 Results

In this section we will present the results of our fit to πN phase shifts using the IAM. Therefore, we will use eq.(9) where t will be now the $L_{2I+1,2J+1}$ partial waves introduced in section 2. The phase shifts are defined customarily from $2iq_{cm}f_{IJ} = e^{2i\delta_{IJ}} - 1$ for the elastic case (see below). Given the large number of free parameters, we have used the MINUIT Function Minimization and Error Analysis routine from the CERN program Library.

The data to which we will fit our amplitudes will be those in [12], which, as commented below, are actually an extrapolation, not including the experimental errors. As it is customarily done with these procedures we will assign an error to the data points in [12]. For instance, in ref.[8] the central points have been given a 3% relative uncertainty. This procedure is not appropriate in our case since we are going to fit data over wide energy ranges, and to use only a constant relative error will give a bigger weight to the data in the low energy regions. Thus we have also added an additional systematic error of 1 degree. ¹ Of course, although the order of magnitude of these errors seems appropriate, the precise values are rather arbitrary, so that the meaning of the $\chi^2/d.o.f.$ obtained from MINUIT has to be interpreted very cautiously. Nevertheless, this error will allow us to use the minimization routine.

Furthermore, as we have commented above, the data near threshold are subject to many uncertainties, so that, also following [8], we will perform all our fits starting from a center of mass energy of $\sqrt{s} = 1130$ MeV (i.e, 150 MeV away from threshold). Therefore, the threshold parameters are really predictions in our approach.

Concerning how high in energies we should try to fit the data, our elastic assumption limits our approach to the energies where inelastic thresholds do not contribute significantly. In particular, the $\pi\pi N$ threshold is at $\sqrt{s} \simeq 1220$ MeV, and we will not use our amplitudes above that energy for the P_{11} , P_{13} and P_{31} partial waves, since their interactions are very weak and the inelastic effects could be significant as soon as the new threshold opens up. The S_{31} and S_{11} phase shifts are larger and we have tried to fit them up to higher energies ($\simeq 1360$ MeV). In other words, we shall restrict to the energy range where the inelasticity parameter, defined through $2iq_{cmt} = \eta e^{2i\delta} - 1$, remains $\eta \simeq 1$. That is why we can fit the P_{33} phase shift up to 1400 MeV.

4.1 The IAM and Resonance Saturation

Following the suggestion that the $O(p^2)$ parameters can be understood from resonance saturation [9], it is natural to try to make an IAM fit keeping their values constant. Thus, we first fix the a_i parameters to the values given in [10], which are compatible with the saturation hypothesis. The $O(p^3)$ parameters resulting from this IAM fit are given in

¹In a very recent paper [15] this approach has been followed with a 5% relative error and a systematic error of $\sqrt{2}$.

Table 2: We give in the first row the results of the IAM, keeping the $\mathcal{O}(q^2)$ values of [10], given in Table 1, which are compatible with the resonance saturation hypothesis. In the second row we display the values from an IAM fit to phase shifts, leaving also the a_i free, but restricted to the ranges predicted with resonance saturation [9] (see Table 1). Let us note that there are strong correlations in the fit so that only certain combinations of the b_i could be meaningful.

	a_1	a_2	a_3	a_5	$b_1 + b_2$	b_3	b_6	$b_{16} - b_{15}$	b_{19}
Fit 1: IAM fit to b_i with a_i fixed to [10] values	-2.6	1.4	-1.0	3.3	28.1	-29.8	2.1	33.3	12.9
Fit 2: IAM fit with a_i restricted to ranges of resonance saturation [9]	-2.1	1.3	-0.8	3.6	22.3	-26.1	2.5	26.7	10.1

Table 2. We used “hatted” quantities, like \hat{b}_i , because their values do not necessarily correspond to those of HBChPT unless there is a good convergence of the low energy expansion, since in our case they are also absorbing the IAM resummation effects and some high energy information. In addition, we also give in Table 2 a second fit where we have allowed the a_i parameters to vary within the ranges expected from the resonance saturation hypothesis (given in Table 1). The results of fit 2 are plotted, as a solid line, in Fig.1.

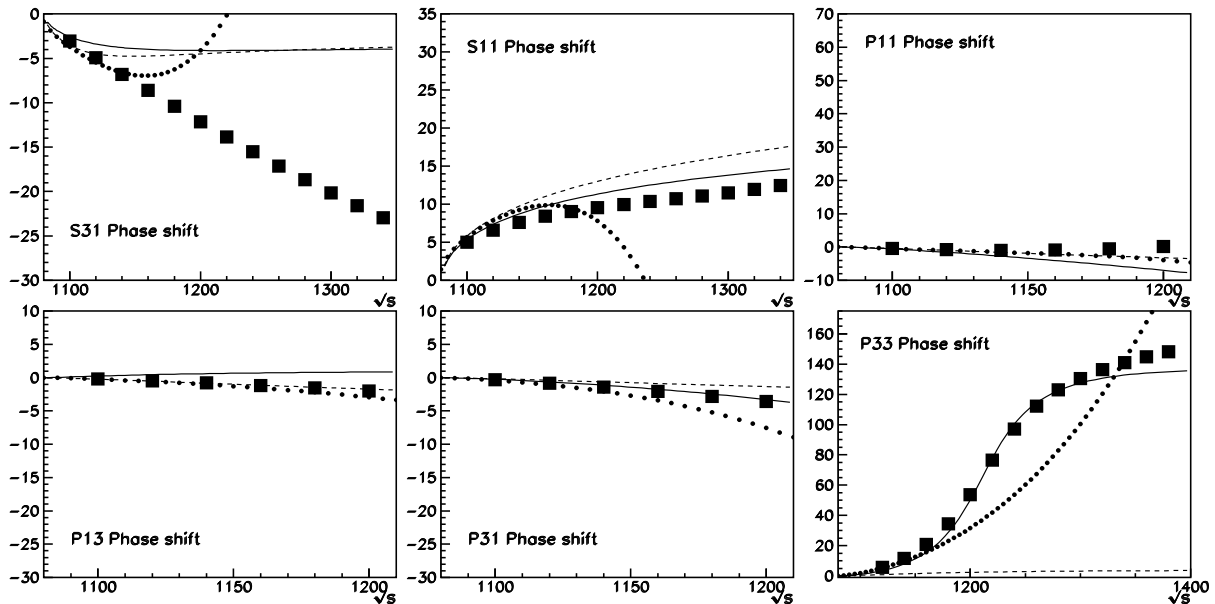


Figure 1: π -N scattering phase shifts. The dotted curve is obtained if we extrapolate to high energies the plain HBChPT result using the chiral parameters of [10]. The dashed line is the prediction of the IAM with the same parameters. Finally, the continuous line is obtained by keeping the a_i parameters within the ranges expected by resonance saturation, and fitting the data with the \hat{b}_i parameters (fit 2). The data come from [12].

Not surprisingly, there are strong correlations between several parameters. Unfortunately, from MINUIT we can only get how strong is the correlation between different parameters, but not its actual form. For example, if we restrict to linear combinations

with integer coefficients, some of them, like $\hat{b}_1 + \hat{b}_2 + \hat{b}_3$ or $\hat{b}_1 + \hat{b}_2 + 2\hat{b}_3 + \hat{b}_{16} - \hat{b}_{15}$, remain within natural sizes for these fits. Nevertheless, as we have commented, there is a considerable uncertainty in the precise values of the b_i at present (see Table 2 in [13]). In addition, as we said before, within our approach, the values of these coefficients are absorbing the effects of the high energy resummation implicit in the IAM. Only if there is a very good convergence of the theory at low energies the values of the low-energy parameters should be similar to those obtained with the IAM (as it happens in ChPT).

Nevertheless, the main conclusion from Fig.1 is that it is possible to obtain a good fit of $\pi - N$ scattering including the $\Delta(1232)$ resonance using the a_i values obtained from resonance saturation. The combinations of \hat{b}_i to which we are sensitive, also yield reasonable values. Note however, that the S_{31} phase shift does not have any real improvement.

For illustration we also give in Fig.1 the extrapolation of the $O(q^3)$ HBChPT results to high energies (dotted line) as well as the IAM result (dashed line), using the [10] values both for a_i and b_i given in Table 1.

4.2 Unconstrained IAM fits

Of course, we can get much better fits by leaving all the parameters free. In such case, and for the error prescription given above we get $\chi^2/d.o.f.$ very close to one. Once more, we get very strong correlations, although their precise expressions are much more difficult to obtain. In Fig.2 we show three different fits, named 3a, 3b and 3c, whose fitted parameters are given in Table 3. Note that the curves are almost indistinguishable. They correspond to some of the many χ^2 minima that we can find in the 9-dimensional parameter space (Indeed, all of them have a $\chi^2/d.o.f. \simeq 0.9$).

Table 3: The IAM can give better fits if we leave the 9 HBChPT parameters free. Unfortunately there are many good fits with rather different values. We only give here those of the fits given in Fig.2. Note that there are strong correlations between different parameters, so that the individual values are not meaningful (see text).

	\hat{a}_1	\hat{a}_2	\hat{a}_3	\hat{a}_5	$\hat{b}_1 + \hat{b}_2$	\hat{b}_3	\hat{b}_6	$\hat{b}_{16} - \hat{b}_{15}$	\hat{b}_{19}
IAM fit 3a	7.40	-7.13	0.68	23.7	0.15	-3.16	0.36	57.57	-19.25
IAM fit 3b	7.30	-7.04	0.67	23.33	10.40	-13.46	0.42	36.55	-19.19
IAM fit 3c	6.33	-7.89	0.2	19.99	-868.45	876.43	4.62	1893.39	-18.33

There are again strong correlations and the actual value of each one of the \hat{a}_i and \hat{b}_i could be rather unnatural. The correlations now are even more complicated due to the quadratic t_2^2 term in the denominator of eq.(9). By inspection of the analytic formulas, we find that the $\hat{a}_1 + \hat{a}_2$, $\hat{a}_5 - 4\hat{a}_1$, $2(\hat{b}_1 + \hat{b}_2) + (\hat{b}_{16} - \hat{b}_{15})$ combinations are the most relevant, and they remain rather stable for these fits. Therefore it is not possible to obtain meaningful values of each individual parameter without any other additional assumption (like resonance saturation).

Let us remark that the $\Delta(1232)$ resonance is clearly reproduced both for the IAM fits in Fig.1 and Fig.2. Indeed the IAM is able to generate dynamically a pole in the second Riemann sheet that we show in Fig.3, whose position, at $\sqrt{s} = (1212 - i47)$ MeV, is rather stable within all the fits, and in very good agreement with the present data [21].

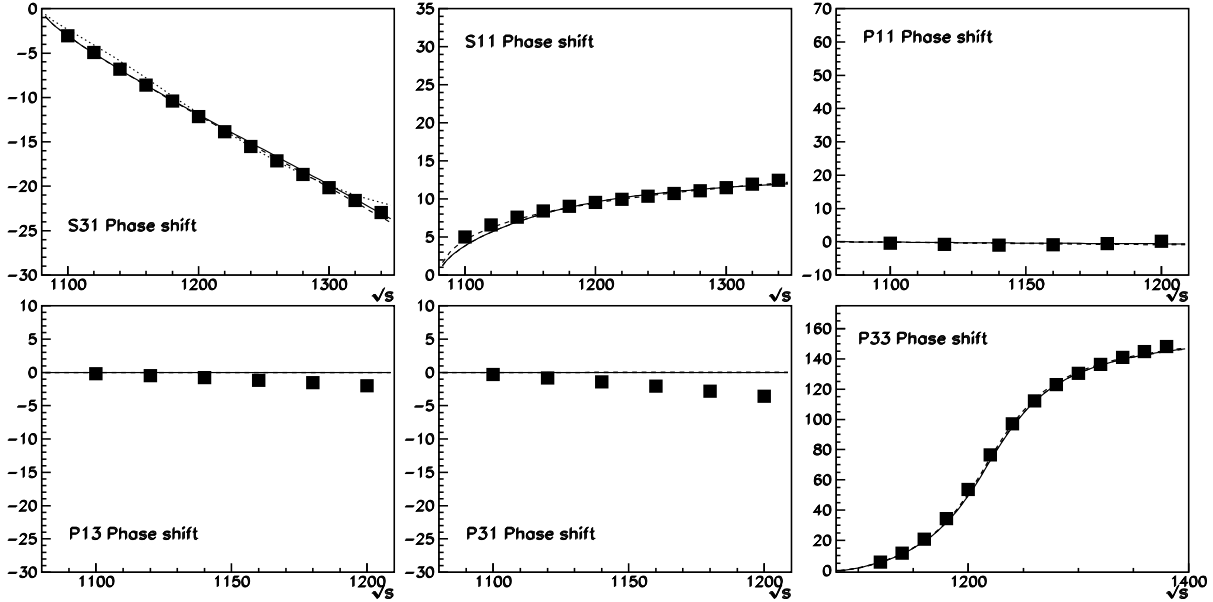


Figure 2: We present here the results of fits 3a (continuous line), fit 3b (dashed line) and 3c (dotted line). Note that, although they are almost indistinguishable, they yield very different chiral parameters (see Table 3). The data come from [12].

In summary, if we leave the 9 parameters free, we can obtain rather good fits, including the $\Delta(1232)$, for very different sets of parameters. That is a consequence of the large number of parameters, but also of the fact that the contributions of different orders in HBChPT are comparable, and a change in any one of them can affect the others, even at a lower order.

4.3 Threshold parameters

Finally, we can predict from our approach the values of the different partial waves and their derivatives at threshold, for the S and P channels. Those values define the scattering lengths and threshold parameters. We shall use again the notation of [10], where we refer for the definitions. The results we obtain for the different fits are shown in Table 3. There, we have also listed the experimental values, extracted from [11]. A word of caution should be said here about the experimental errors. As pointed out in [11] and [10], those errors are clearly *underestimated*, because they are extrapolations. Therefore, it should be borne in mind that the scattering lengths are not so well determined as it may seem from those errors (see also the discussion in [8]). We see that our fits give a reasonably good agreement with experiment for the S -wave scattering lengths. The results are not so good for the P -wave, although in most cases we agree with the order of magnitude and sign. Our results are also roughly in agreement with [8], where, for instance, the following values for the S -wave scattering lengths are obtained: $-0.07 \text{ GeV}^{-1} \leq a_0^+ \leq 0.04 \text{ GeV}^{-1}$ and $0.6 \text{ GeV}^{-1} \leq a_0^- \leq 0.67 \text{ GeV}^{-1}$.

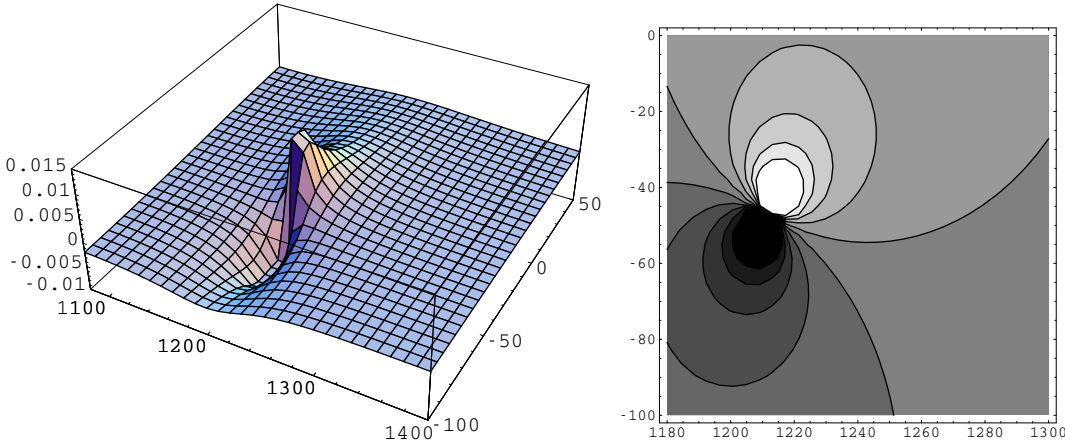


Figure 3: Position of the $\Delta(1232)$ pole in the second Riemann sheet.

5 Conclusions and discussion

By using the Inverse Amplitude Method, we have been able to unitarize the $\pi - N$ elastic scattering amplitude obtained from HBChPT to $\mathcal{O}(q^3)$. This procedure allows to fit the phase shifts for the partial waves up to the inelastic thresholds and, in addition, it gives the right pole for the $\Delta(1232)$ in the P_{33} channel. Our fitting method consisted in using the extrapolated phase shift data between a center of mass energy of $\sqrt{s} = 1130$ MeV and the corresponding inelastic thresholds. Within this approach, we can predict the thresholds values, which, at least for the S waves are in good agreement with experiment and with recent determinations.

Unfortunately, since there are large correlations between some parameters, it is possible to obtain good fits with rather different sets of parameters. This fact is due to different reasons: a) The slow convergence of the series. Indeed we have checked that contributions from different orders are comparable in almost every partial wave at the energies we use. The effect of higher order terms, which was less relevant at threshold, is absorbed in our case in the values of the chiral coefficients. b) There are strong correlations between the parameters, so that the fits are only sensitive to certain combinations and not to the precise values of each individual coefficient.

One of the relevant conclusions of this study is that we can still reproduce the $\Delta(1232)$ with the a_i values expected from the resonance saturation hypothesis, keeping a reasonably good description for the other channels.

Finally, we would like to remark that the method developed here can be easily extended to the case of $SU(3)$ symmetry as well as to the coupled channel formalism. Further work along these lines is in progress.

Table 4: Threshold values for the S and P -wave amplitudes (scattering lengths) with the different IAM fits, compared with the experimental values in [11] (see text). Fit 2 is constrained to have a_i values within the ranges of resonance saturation. Fit 3 is totally unconstrained.

	Extrapolated from Experiment	IAM constrained to resonance saturation (fit 2)	IAM unconstrained (fits 3)
a_0^+ (GeV $^{-1}$)	-0.07 ± 0.01	0.02	-0.12
a_0^- (GeV $^{-1}$)	0.67 ± 0.1	0.72	0.53
b_0^+ (GeV $^{-3}$)	-16.9 ± 2.5	-2.8	-16.43
b_0^- (GeV $^{-3}$)	5.1 ± 2.3	-9.0	13.59
a_{1+}^+ (GeV $^{-3}$)	50.5 ± 0.5	41.04	79.08
a_{1-}^+ (GeV $^{-3}$)	-21.6 ± 0.5	-18.35	-2.09
a_{1+}^- (GeV $^{-3}$)	-31.0 ± 0.6	-11.52	-39.58
a_{1-}^- (GeV $^{-3}$)	-4.4 ± 0.4	-6.75	-2.00

Acknowledgments

Work partially supported by DGICYT under contract AEN97-1693. J.R.P. thanks J.A.Oller and E.Oset for useful discussions.

References

- [1] E. Jenkins and A. V. Manohar, Phys. Lett. B255 (1991) 558; V. Bernard, N. Kaiser, J.Kambor and U. -G. Meißner, Nucl. Phys. B388 (1992) 315. G. Ecker, Czech. J. Phys. 44 (1994) 405; V. Bernard, N. Kaiser and U. -G. Meißner, *Int. J. Mod. Phys.* **E4** (1995) 193.
- [2] E. Jenkins and A. V. Manohar, Phys. Lett. B259 (1991) 353
- [3] S. Weinberg, *Physica* A96 (1979) 327; J.Gasser and H.Leutwyler, Ann. Phys. 158 (1984) 142, Nucl. Phys. B250 (1985) 465.
- [4] J. Gasser, M. E. Sainio and A. Svarc, Nucl. Phys. B307 (1988) 779.
- [5] T.Mannel, W.Roberts and Z.Ryzak, Nucl. Phys. B368 (1992) 315.
- [6] H. Georgi, Phys. Lett. B240 (1990) 447.
- [7] G. Ecker and M. Mojzis, Phys. Lett. B365 (1996) 312.
- [8] N.Fettes, U.-G. Meißner and S. Steininger, Nucl. Phys. A (1998) 199.
- [9] V. Bernard, N. Kaiser and U. -G. Meißner, Phys. Lett. B309 (1993) 421; Phys. Rev. C52 (1995) 2185; Phys. Lett. B389 (1996) 144; Nucl. Phys. A615 (1997) 483;
- [10] M. Mojzis, Eur. Phys J. C 2 (1998) 181.
- [11] R.Koch and E.Pietarinen, Nucl. Phys. A336 (1980) 331.
- [12] R. Arndt et al. nucl-th/9807087. SAID online-program.(Virginia Tech Partial-Wave Analysis Facility). Latest update, <http://said.phys.vt.edu>.

- [13] P. Büttiker and U.-G. Meißner, [hep-ph/9908247](#).
- [14] A. Datta and S. Pakvasa, Phys. Rev. D56 (1997) 4322; P.J. Ellis and H.-B. Tang, Phys. Rev. C57 (1998) 3356.
- [15] U-G. Meißner and J. A. Oller, [nucl-th/9912026](#).
- [16] T. N. Truong, Phys. Rev. Lett. 661 (1988) 2526; Phys. Rev. Lett. 67 (1991) 2260; A. Dobado, M.J.Herrero and T.N. Truong, Phys. Lett. B235 (1990) 134 ; A. Dobado and J.R. Peláez, Phys. Rev. D47 4883 (1993); Phys. Rev. D56 (1997) 3057.
- [17] J.A. Oller, E. Oset and J.R. Peláez, Phys. Rev. Lett. 80 (1998) 3452 ; Phys. Rev. D59 (1999) 074001; [hep-ph/9909556](#). F. Guerrero and J. A. Oller, Nucl. Phys. B537 (1999) 459.
- [18] T. Ericson and W. Weise, *Pions and Nuclei*, Oxford 1988 and references therein.
- [19] J.L. Basdevant, Fort. der Phys. 20 (1972) 283.
- [20] E. Oset and A. Ramos, Nucl. Phys. A635 (1998) 99.
- [21] *Review of Particle Physics*, Particle Data Group, Eur. Phys. J. C3 (1998) 1.